The Near Earth Object (NEO) Scout Spacecraft: A low-cost approach to in-situ characterization of the NEO population

Eric A. Woeppel,[1] James M. Balsamo,[1] Karl J. Fischer,[1] Matthew J. East,[1]
Jeremy A. Styborski,[1] Christopher A. Roche,[1] Mackenzie D. Ott,[1] Matthew J. Scorza,[1]
Christopher D. Doherty, [1] Andrew J. Trovato,[1] and Christopher P. Volk[1]
Rensselaer Polytechnic Institute, Troy, NY, 12180, USA

Dr. Steven L. Koontz[2]
NASA JSC, Houston, TX, 77058, USA

Dr. Riccardo Bevilacqua[3]
Rensselaer Polytechnic Institute, Troy, NY, 12180, USA

Dr. Charles Swenson[4]
Utah State University, Logan, Utah 84322-1400, USA

This paper describes a microsatellite spacecraft with supporting mission profile and architecture, designed to enable preliminary in-situ characterization of a significant number of Near Earth Objects (NEOs) at reasonably low cost. The spacecraft will be referred to as the NEO-Scout. NEO-Scout spacecraft are to be placed in Geosynchronous Equatorial Orbit (GEO), cis-lunar space, or on earth escape trajectories as secondary payloads on launch vehicles headed for GEO or beyond, and will begin their mission after deployment from the launcher. A distinguishing key feature of the NEO-Scout system is to design the spacecraft and mission timeline so as to enable rendezvous with and landing on the target NEO during NEO close approach (<0.3 AU) to the Earth-Moon system using low-thrust/high-impulse propulsion systems. Mission durations are on the order 100 to 400 days. Mission feasibility and preliminary design analysis are presented, along with detailed trajectory calculations.

Nomenclature

NEO	=	Near Earth Object
GEO	=	Geosynchronous Equatorial Orbit
1U	=	a standard unit for CubeSats, 10x10x10cm^3
NASA JPL	=	National Aeronautics and Space Administration Jet Propulsion Laboratory
NHATS	=	Near-earth object Human space flight Accessible Targets Study
delta V	=	Change in velocity after impulse, km/s
COTS	=	Commercial Off-The-Shelf
AU	=	Astronomical Unit, 149,597,870.700 kilometers
STK	=	System Tool Kit
RCS	=	Reaction Control System
Isp	=	Specific Impulse, s
PMS	=	Propellant Management System
ADCS	=	Attitude Determination and Control System
CPU	=	Central Processing Unit
X_i, Y_i, Z_i	=	Axis used where subscript i denotes the reference frame

[1] Senior Design Project Student, Mechanical Aerospace and Nuclear Engineering Department, Rensselaer Polytechnic Institute, Troy, NY, 12180, USA, AIAA Student Member

[2] International Space Station System Manager for Space Environments, NASA JSC, Houston, TX, 77058, USA, AIAA Member

[3] Associate Professor, Mechanical Aerospace and Nuclear Engineering Department, Rensselaer Polytechnic Institute, Troy, NY, 12180, USA, AIAA Member

[4] Associate Professor, Department of Electrical and Computer Engineering, Utah State University, Logan, Utah 84322-1400, USA, AIAA Member

i=Body = Satellite's body centered reference frame
i=SP = Solar Panel's centered reference frame
PV = PhotoVoltaic
PDM = Power Distribution Module
UTJ = Ultra Triple Junction
PPU = Power Processing Unit
SBIR = Small Business Innovation Research
DSN = Deep Space Network
SPE = Single Particle Event
bps = bits per second
e_1 = charge of the projectile (proton), $1.602176 \cdot 10^{-6}$ C
E = elementary charge, $1.602176 \cdot 10^{-6}$ C
Z_2 = atomic number of material
M = mass of an electron, $9.10938291 \cdot 10^{-31}$ kg
V = speed of light, 299,792,458 m/s
I = mean logarithmic excitation energy of stopping material
ESA = European Space Agency
ISS = International Space Station
LEO = Low Earth Orbit

I. Introduction

The use of microsatellites in low-cost interplanetary exploration is attracting increasing attention and is the subject of several annual workshops and published design studies.[1–4] The NEO population consists of asteroids and short period comets orbiting the Sun with a perihelion of 1.3 astronomical units or less.[5–8] As of July 30, 2013, 10065 Near-Earth objects have been discovered. The dimensions, spin rate, mass, density, surface physical (especially mechanical) properties, composition, and mineralogy of the vast majority of these objects are highly uncertain, and the limited available telescopic remote sensing data imply a very diverse population.[5–8] In-situ measurements by small low-cost robotic spacecraft are urgently needed to provide the characterization data needed to support high-confidence hardware and mission design for more ambitious human and robotic NEO operations.

Large numbers of NEOs move into close proximity with the Earth-Moon system every year.[9] The JPL Near-Earth Object Human Space Flight Accessible Targets Study (NHATS)[10] has produced detailed mission profile and delta V requirements for various manned NEO missions ranging from 30 to 420 days in duration, assuming chemical propulsion. Similar studies have been reported assuming high power electric propulsion for manned NEO rendezvous missions.[11] The delta V requirement breakdown and mission profile data from references 10 and 11 are used as a basis for sizing the NEO-Scout spacecraft and conducting preliminary feasibility assessments using the Tsiolkovsky rocket equation, a maximum delta V requirement of 10 km/s, and a maximum spacecraft dry mass of 20 kg. Using chemical propellant for a 10 km/s delta V drives the spacecraft's wet mass to well above 300 kg so that chemical propulsion is a non-starter for the proposed mission profile and the spacecraft's wet mass limits. In contrast, the solar electric propulsion system needs only 10 kg of iodine propellant to accelerate the spacecraft with a dry mass of 20 kg to 6.3 km/s in 47 days with 0.039 N of thrust and 600 W of photovoltaic power.

The cost of reaching space has historically proved a barrier that only the most well-funded government agencies are able to overcome. Recently, a movement to find a low-cost yet effective method of putting a device into orbit has given birth to the widespread use of the CubeSat, a miniature satellite defined by 10 cm cube units called the 1U cube.[12] Small size and prudent use of Commercial Off-The-Shelf (COTS) components where possible can make CubeSats up to 2 orders of magnitude less costly than conventional spacecraft allowing for large numbers to be deployed as constellations to survey large volumes of space. Originally created by Professor Robert Twiggs of Stanford University, the CubeSat provides a way for a low budget mission to share flight costs with a larger customer and successfully place hardware in orbit.[13] Because the NEO population is large and diverse, multiple, low cost spacecraft are required to characterize the population.

A NEO-Scout spacecraft program can provide valuable preliminary target selection and characterization data in comparison to a larger, costlier, and more capable spacecraft like Hayabusa. This particular mission provided validation of ground based asteroid research methods and successfully implemented long term use of an ion engine. Through the close up observation of the asteroid, 25143 Itokawa, Hayabusa was able to provide valuable information to scientists about near Earth asteroids as well as return samples. However, the Hayabusa spacecraft cost over $100 million and took seven years to complete its mission to study one asteroid at a total program cost of about $400 million.[14]

In this paper, we report a design and feasibility assessment of the NEO-Scout spacecraft. Based on CubeSat technology, the NEO-Scout spacecraft can enable preliminary characterization of a large number of NEOs within a reasonably short period of time and at relatively low cost. The work presented below constitutes proof of concept for one possible design solution thought by the authors to meet the mission requirements in the most efficient way.

II. The NEO-Scout Spacecraft Performance Requirements

In the following sections, the feasibility of a microsatellite rendezvous mission is discussed. A relatively challenging NEO target was selected to demonstrate the robustness of the NEO-Scout concept model. The following sections show characteristics of a low-thrust trajectory for rendezvous with the target within the 400 day mission duration limit while minimizing the cost and weight. High level NEO-Scout performance requirements and general characteristics are summarized in Table 1 below.

The spacecraft dry weight limit is first combined with the maximum delta V requirement of 10 km/s in the Tsiolkovsky rocket equation to calculate required propellant mass as a function of thruster specific impulse to select the type of thruster that would be able to meet the wet mass requirement. Only high specific impulse electrostatic ion engines and Hall Effect thrusters could meet the wet mass requirements for a 10 km/s delta V and a 35 kg maximum wet mass.

Next a survey of commercially available high impulse satellite thrusters was conducted to identify possible candidates for the NEO-Scout spacecraft design. An additional constraint appears at this point driven by the maximum mission duration limits. The NEO-Scout thrust-to-weight ratio needs to be high enough to enable acceleration to the desired final velocity within the allotted mission time.

The focus of the design effort involved determining whether or not the remaining spacecraft system could be assembled into an integrated functional spacecraft that conformed to the general requirements without violating the maximum wet mass limits. The design was further refined and optimized to meet the more specific delta V and trajectory requirements for the target NEO selected for this study; however, the spacecraft body and subsystems are able to stay relatively consistent with changes to payloads depending on mission specific requriements.

Table 1. NEO-Scout Spacecraft General Requirements and Characteristics.

Dry Mass Range	< 20 kg
Wet Mass Range	< 35 kg
Delta V Range	< 10 km/s
Maximum Mission Duration	100 to 400 days
Maximum Distance to Earth at Rendezvous	0.3 AU
Maximum Telemetry Range	0.3 AU
Minimum Telemetry Data Rate	2000 to 10000 Bps
Spacecraft Unit Cost	$15M

III. NEO Target Selection

To find NEOs whose orbit enables a rendezvous trajectory within the constraints of the NEO-Scout requirements, NASA's planetary databases were used.[8–10] This database includes all known NEO orbital elements and lists possible rendezvous trajectories using an impulsive Lamberts Problem solver. Due to the large number of NEOs, Table 12 in the appendix was created from the asteroids which fall under the constraints in Table 2. From these, the 2007 SQ6 was chosen and is presented in Table 2 as well.

Table 2. NEO Target Selection Constraints and selected target's values.

Variable	Value	2007 SQ6
Launch Epoch, Date	Jan. 1, 2020 to Jan. 1, 2025	Sept. 29, 2023
NHAT Flight Time, Days	≤ 400	96
Closest Approach, AU	≤ 0.15	0.00982
Inclination, Degrees	≤ 10	9.101
Eccentricity	≤ 0.15	0.1456
Semi-Major axis, AU	0.7 – 1.3	1.0430
Size, m	≥ 100	111-248

Due to Earth's nearly circular orbit, the optimum time of launch depends almost entirely on the orbit of the asteroid. Using the Keplerian method of orbit determination, the most important variables for identifying a possible target are the NEOs inclination, eccentricity, and semi-major axis. The inclination is representative of the maximum efficiency of a trajectory due to the necessary thrust to perform the inclination change. In addition, with a low

inclination, the longitude of ascension argument of perigee will not make a significant difference in the trajectory due to the near-circular orbit of Earth.

With transmitter size and power limitations of microsatellites, the closest approach was set to less than 0.15 AU. The close proximity to Earth allows for higher data transfer rates. Flight time is limited to one year both to decrease risks associated with space radiation effects on NEO-Scout avionics reliability and to increase rate of data return while minimizing mission operations cost. However, limiting flight time also negates the option of conducting planetary gravity assist maneuvers that are often an essential feature of Discovery class robotic missions. Such maneuvers are not effective for the target NEOs, as it would take more time and energy to go to another planet then a direct trajectory to the asteroid. That being said, a lunar gravity assist could provide a delta V boost of about 0.5 km/s and decrease the need for on-board fuel.

The 2007 SQ6 rendezvous trajectory reported here constitutes proof of concept that low thrust microsatellites will be able to rendezvous with asteroids that are not optimal targets, and therefore proves that low thrust microsatellite exploration of the NEO population is possible. 2007 SQ6 was selected, not because it is an easy target, but instead because it is difficult to reach. Another NEO which has already been a target of studies is 2004 MN4, better known as Apophis. Trajectories and mission proposals have been worked out for larger satellites to rendezvous with Apophis, such as the one proposed in SpaceWorks' Foresight proposal in 2008.[15] Unfortunately, these missions have not been conducted due to budgeting issues and time constraints, but is achievable with the NEO-Scout approach.

IV. Trajectory

NEO-Scout missions will utilize low-thrust/high-impulse Hall Effect thrusters and therefore will fly different trajectories than those found in the NASA database, which assumes impulsive trajectories. However, the impulsive trajectory data proved useful as a source of initialization data for iterative low-thrust trajectory optimization for the NEO-Scout flights. The trajectories used in this paper were found using the program Systems Tool Kit (STK).[16] The iterative differential corrector targeting profiles, found in the STK Astrogator propagator, allows trajectories to be calculated given constant or variable initial, final, and stopping conditions for each trajectory segment. The trajectory selected is shown in Figure 1. The sequence of engine burns required by this trajectory is described in Table 3 below.

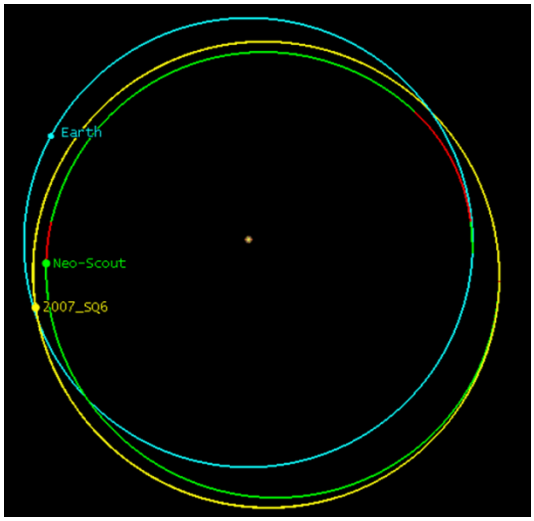

Figure 1. Locations on 17 February, 2023 and planned trajectory for rendezvous trajectory with 2007 SQ6

While there are more optimum trajectories for 2007 SQ6, the one presented was chosen to optimize data transmission. Rendezvous occurs 7 days before a 78 day span where the NEO will remain within 0.15 AU of Earth. This allows for system checks before beginning data acquisition. Due to the close proximity, the data transfer rate will be well above the minimum required. This enables the return of higher resolution imagery in shorter periods of time as, described in the communications section of this paper.

Table 3. Engine Burn Sequence for 2007-SQ6 Neo-Scout Rendezvous Trajectory.

Engine Burn	Epoch Engine Burn Start	Epoch Engine Burn Stop	Delta V, m/s	Propellant Consumption, kg	Reason for Burn
1	23 Sept. 2022 06:58 UTC	25, Oct, 2022 04:19 UTC	5153.07	6.913	Inclination Change; Lower Periapsis; Raise Apoapsis
2	7 Feb. 2023 02:31 UTC	16 Feb, 2023 09:51 UTC	1893.81	2.017	Raise apoasis and apse line change
3	31 Aug. 2023 16:50 UTC	3 Sep. 2023 00:00 UTC	663.26	0.544	Orbit matching by raising periapsis
Total	23 Sept. 2022, 06:58 UTC	3 Sep. 2023, 00:00 UTC	7680.33	9.474	2007 SQ6 Rendezvous

A. Initial State and Earth Escape

Due to the wet mass requirements, an additional chemical engine burn by the launch vehicle upper stage is needed. As with the NEAR Shoemaker mission,[17] it was decided that the launch vehicle would provide an initial heliocentric orbit. This is achievable via a multi-staged Delta class rocket. The point of Earth departure was chosen to be the Sun-Earth L_1. This point was chosen because the semi-major axis needed to decrease as part of an initial "catch up" maneuver. Lagrange points 1 and 2 act as libration points for the Sun-Earth system, minimizing the necessary energy to exit Earth's orbit.

B. Interplanetary Trajectory Correction Maneuvers

Three finite burns were conducted over the 346 days of interplanetary flight. It can be seen that there is a large difference in flight times between the 96 day impulsive trajectory found in the NHAT data base and the low-thrust 346 day NEO-Scout trajectory. This is because, for larger inclination changes, an impulsive solution is able to change inclination immediately, while the finite maneuvers require an increased amount of time to reach the necessary velocity change. Inclination changes are impulsively optimal during the crossing of planes of the current and target orbits. For finite duration, low-thrust burns, the impulsive trajectory times can only act as a reference for where the maneuver should be. As a result, the inclination maneuver requires a large thrust angle with respect to the velocity vector to complete the inclination change within the optimal region.

C. Proximity Maneuvers

Taking the maximum estimated diameter of 2007 SQ6, 248 meters, and an assumed density of 2500 kg/m^3, the surface gravitational acceleration (assuming a spherical geometry) is 8.7 x 10^{-5} (m/s^2)[8–10] implying a near surface orbital velocity of only 10.4 cm/s and an escape velocity of 14.7 cm/s. Since there is currently no shape model of 2007 SQ6, a scale model of 433 Eros with maximum diameter of 248 meters is used for the asteroid proximity simulation.

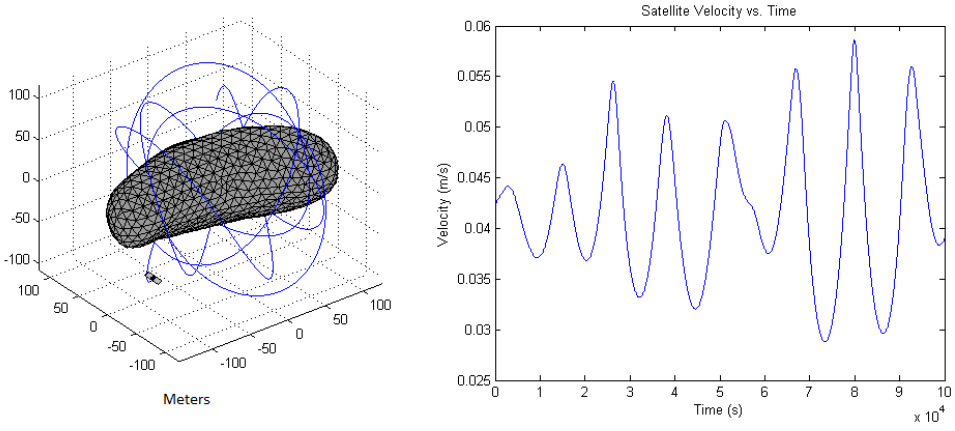

(a) **(b)**

Figure 2a. Shown in 1:7.6 scale of NEO-Scout to asteroid, the NEO-Scout is in a Passive Orbit over 1.157 days with initial velocity. Figure 2b. Shows the velocity as a function of flight time.

After rendezvous, NEO-Scout will need to conduct proximity maneuvers close to the surface of 2007 SQ6. As seen in the passive orbit above, the irregular shape of asteroids causes abnormal accelerations. Due to these, once rendezvous has occurred the satellite will need active control to insure the satellite does not crash before its mission is completed. Such maneuvers were successfully conducted during the Hayabusa mission to Itokawa, which had a similar surface gravity. These maneuvers were incredibly precise enabling Hayabusa to hover above the rotating surface at heights of 7 meters.[18,19] NEO-Scout will use cold gas thrusters with 0.050 N of thrust and will provide the thrust for orbit matching and proximity maneuvers about 2007 SQ6. A simulation of the NEO-Scout station keeping at 60 meters and taking off from the surface using two cold gas thrusters are included in Figure 3. It should be noted that four cold gas thrusters will be available during the mission; however, the limiting factor for number of close approaches is the mass of N_2.

As seen in Figure 3, NEO-Scout will be more than able to land on and launch from 2007 SQ6. Given the mission parameters, a larger N_2 tank can be equipped to enable a longer maneuverable life. Station keeping at a higher altitude would decrease the fuel needed to maintain a stationary position, with respect to the asteroid. That being said, there is a Lagrangian point where the satellite would be able to rest with minimal energy and observe the asteroid before beginning proximity maneuvers. Stable orbits can be found in-situ through the use of on board

instrumentation. These orbits would be used to acquire data on asteroid shape and angular velocity to transmit to Earth as well as to mitigate the risk of impact failure. If landing is desired, the satellite will be able to launch from the asteroid to escape velocity with 25 s of cold gas thrust, or much less for orbit injection.

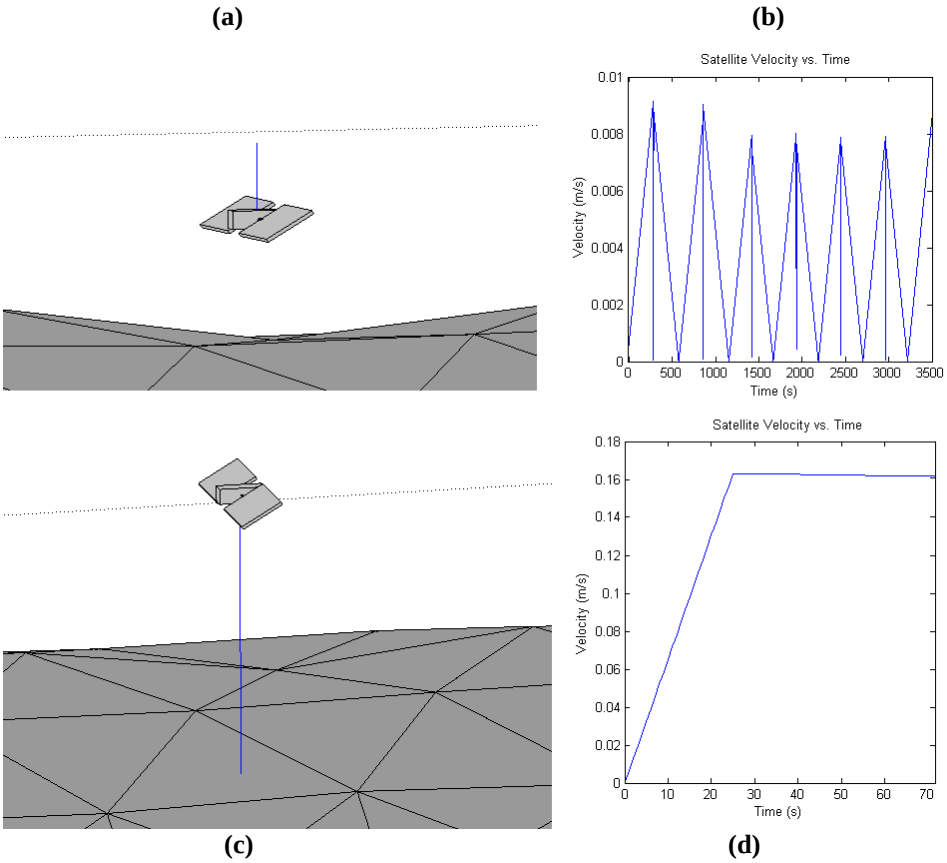

Figure 3a. Station keeping trajectory. Figure 3b. Station keeping velocity profile. Figure 3c. Asteroid launch trajectory. Figure 3d. Asteroid launch velocity profile.

V. Main Propulsion

The Tsiolkovsky rocket equation was used to estimate propellant mass as a function of the propulsion system's specific impulse for a 20 kg spacecraft dry weight and a delta V of 10 km/s. The lower specific impulse of high-thrust chemical propulsion systems requires a total propellant mass of more than 300 kg, while for the much higher impulse of low-thrust electric propulsion systems, propellant mass was less than 10 kg. Since the NEO-Scout mission concept allows for 100 to 400 days duration with departure from a starting point at or beyond GEO, there is no need for high-thrust chemical engines after the launch vehicle has placed the NEO-Scout at or near the departure point. Ion engines, such as electrostatic ion thrusters and Hall-effect thrusters, typically operate at high specific impulses and low thrusts.[20] Due to this, they are the preferred choice for the small satellite missions described here.

A. Engine Selection

Electrostatic ion engines typically provide specific impulse on the order of 3000 s while a Hall effect engine's specific impulse is on the order of 1500 s. Electrostatic engines appear to offer an advantage over Hall Effect engines because the higher impulse leads to reduced propellant mass. This advantage is offset by the complexity and mass of the flow control for the electrostatic thruster system. In contrast, Hall effect thrusters offer favorable thrust and mass while decreasing specific impulse. More importantly, Hall effect thrusters have been proven to operate on fuels besides xenon. Iodine, specifically, has been shown to operate in a manner similar to Xenon and can be stored at higher densities and lower pressures.[21,22]

To select the main propulsion Hall effect thruster for the craft, an extensive search was conducted on commercially available Hall effect thrusters.[23-28] Busek produces a Hall effect thruster, the BHT-600, which provides a nominal thrust of 39 mN at a power input of 600 W. Table 4 lists the values of thrust, specific impulse, power input range, mass, and proven fuels for the Busek engine. All values depicted are drawn from the manufacturer's website.[23] With current technology, the combined mass of the thruster and the associated power

processing unit is 4.3 kg. Note that the mass column denotes the combined mass goal of the thruster and power processing unit based on the SBIR development goal.[25] The BHT-600 has been proven to operate with multiple propellants.[23] Iodine has advantages over xenon in terms of storage, flow control, and maximum charge.

Any parameters relevant to the mission modeling, such as fuel mass flow rate and wet-to-dry mass ratio, can be approximately calculated from the nominal values given in Table 4. More comprehensive performance figures for the BHT-600 can be obtained from experimental studies.[26,27] A NEO-Scout spacecraft with 20 kg dry mass can provide a delta V of 7.7 km/s in 47 days using the BHT-600 engine and 9.5 kg of propellant.

Table 4. Busek BHT-600 Hall Effect Thruster Performance Characteristics

Engine	Tested Fuels	Thrust, mN	I_{sp}, s	Power Input, W	Mass, kg
Busek BHT-600	Xe, Ar, Kr, I, Bi, Zn, Mg	39 (at 600W)	1585 (at 600W)	300-800	3

The possibility of a change in the spacecraft's center of mass during flight implies that an off-center thrust could be generated. The off-center thrust would create a torque about the center of mass which must be counteracted by the use of cold-gas thrusters or reaction wheels. Another possible remedy is engine gimbaling. Changing the thrust vector of the BHT-600 would allow the thrust axis to remain in line with the center of mass; if needed, the gimbal system could also be used to provide attitude control. For a CubeSat configuration of 2Ux3Ux1U and a center of mass at the volumetric center, the center of mass can vary by roughly 0.3 cm per degree of gimballing angle and still lie along the thrust line. Similarly, for a center of mass that remains at the volumetric center, roughly 0.12 mN·m of torque per degree of gimballing angle is produced. At the moment, only one COTS CubeSat gimbaling system, the COBRA Gimbal from Tethers Unlimited, has been identified.[29]

B. Propellant Management System

The Propellant Management System (PMS) for the NEO-Scout spacecraft was designed for the use of iodine as propellant. This gives this system mass and volume advantages over previously flown electric propulsion systems. The subsystem also incorporates controls to achieve the operating conditions required by iodine.

Iodine can be stored as a solid at ambient temperatures and is easily sublimed through heating. This enables a propellant tank to store iodine at minimal volume, 1 L for a 5 kg mass, and low pressure, less than 15 psi. These values are very favorable when compared to similar propellant mass xenon systems which could require 3 L and greater than 1000 psi storage respectively.[30] The low operating pressure enables the use of standard aluminum alloys for tank construction, with a resistant lining to prevent corrosion. This system utilizes a 2U aluminum rectangular prism for iodine storage. The cube is covered in Tempco etched foil element Kapton heaters to provide the necessary heating to sublimate the iodine for use.[31] A conservative estimate for the mass of the tank and heaters is 0.5 kg.

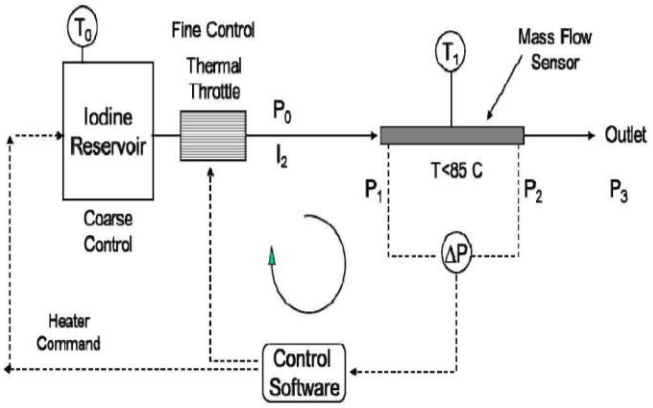

Figure 4. An example iodine flow control system, detailing feedback inputs and outputs.

Additional mass savings are achieved through the simplification of the gas flow control system. At high storage pressures, xenon requires complex components to achieve accurate control. Iodine flow control can be achieved primarily through heater based flow regulation. The iodine reservoir is heated to approximately 80°C to increase pressure.[32] Pressure transducers downstream measure pressure drop along with thermocouples determining gas temperature. Mass flow can then be calculated based on pipe geometry and gas properties. Finer flow to the engine anode and cathode can be achieved through the use of thermal throttles. A block diagram of this system can be seen in Figure 4.[33]

For the BHT-600, a normal operational mass flow rate of 2.6 mg/s from the tank is expected.[34] If the fuel lines are not properly heated, the gaseous iodine will create solid deposits throughout the system. This PMS is designed to heat feed lines to approximately 150℃ through the use of the Tempco Kapton heaters.[32] The Kapton heaters were selected based on their low mass and ability to satisfy thermal and power requirements.

VI. Attitude Control and Proximity Operations

An Attitude Determination and Control System (ADCS) is required in order to ensure stability of the NEO-Scout throughout the mission. For this design, the software used to control the orientation of the spacecraft in orbit around the Earth or Sun is one of the most crucial and sensitive subsystems aboard the craft. The purpose of the attitude control software is to interpret position, orientation, and acceleration data from the star tracker, determine the inertia profile of the spacecraft, and send control signals to the orientation control hardware that would move the craft into its desired alignment. In a mission where the destination is a relatively small body millions of kilometers from Earth, small errors in orientation control could lead to large errors in trajectory, due to the fact that the thrust vector is fixed by the spacecraft attitude. To achieve this, two different control systems were employed. Reaction wheels provide a slow, precise orientation change which becomes critical when employing lengthy finite burns when precision of orientation greatly affects the resulting trajectory. A system of cold gas thrusters was also selected for quick response proximity maneuvers around the asteroid. These thrusters also provide redundancy for the reaction wheels and are able to desaturate if the maximum rotational velocity is reached.

A. Orientation Determination

The reaction wheel module selected was the Blue Canyon Technologies XACT.[35] This 0.5 U micro-package has 3-axis control reaction wheels as well as a star tracker. The XACT was selected for its lightweight and integration of navigation with the internal CPU for autonomy, see Section X on Computing. The first step in this process is to find the position of the vehicle using a star tracker. By correlating images of known constellations, the star tracker can provide an accurate position, orientation, and body angular velocity for the craft in its orbit around the central body. Convergence time for a lost in space solution is rated at 2 seconds.

After integration of the star tracker with the internal CPU, the NEO-Scout needs to align the actual and desired body reference frames. This is shown in Figure 5a and 5b respectively. The X_{body} vector is defined as the direction of actual thrust and Z_{body} is defined normal to the front of the craft. Y_{body} is defined by the cross product of the Z and X axis. At any position, it is desired that X_{body} aligns with the thrust vector so that the Z_{body} axis lies within the position-thrust plane (allowing Y to lie perpendicular to it). The spacecraft desired orientation is determined by two vectors. Since the main method of propulsion is fixed to the spacecraft, the thrust vector is fixed relative to the body. The thrust vector is determined by the desired trajectory. Spacecraft orientation is also partially determined by the position vector to the Sun since it is solar powered. Both the Sun position vector and the desired trajectory can also be determined from information provided by a device such as a star tracker.

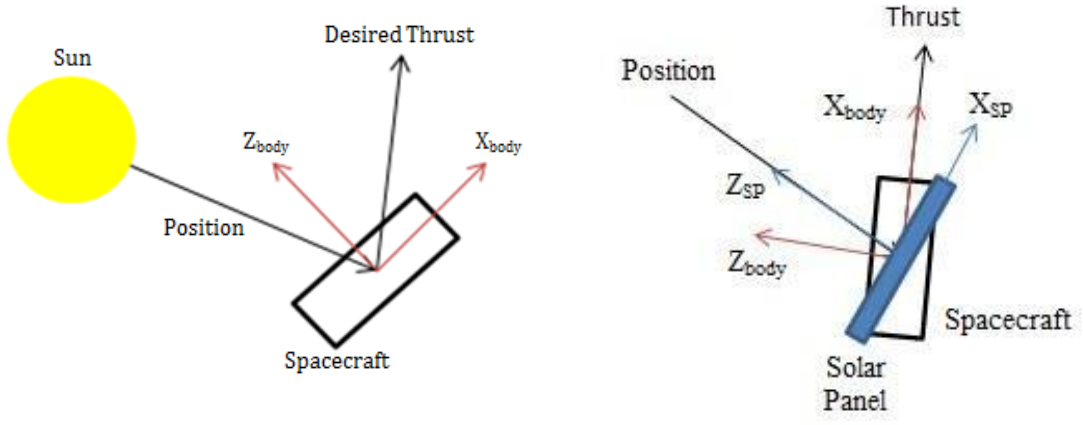

(a) **(b)**

Figure 5a (left). Spacecraft Orientation in Space Using Desired Vectors and Body-Fixed Axes. Figure 5b (right). Spacecraft and Solar Panel Orientation along the Desired Thrust and Desired Position Vectors respectively.

The spacecraft solar panels operate optimally when directly facing the Sun. Since the radial solar panels are designed to rotate about the Y_{body} axis, in a posigrade orbit they will always be able to face the Sun with $\pm 90°$ rotational freedom. Figure 5b shows the spacecraft aligned with the desired thrust vector and its rotating solar panels aligned with the desired position vector. When the actual and desired orientations are compared an error is generated. This error is sent to the Power Distribution Module (PDM) in the form of a request for a voltage. The PDM then sends the required voltages to the Micro 3-Axis Reaction Wheels to correct the calculated error. If the torque required exceeds the maximum, coordination with cold gas thrusters is required to provide the additional

force. In addition, if the reaction wheels reach a terminal angular velocity, then cold gas thrusters are used to desaturate the wheels.

B. Reaction Wheel Desaturation and Proximity Operations

For the NEO-Scout design, the cold gas thrusters will be used for assisting with attitude control, translational maneuvers, and desaturation of reaction wheels. Twelve cold gas thrusters will be attached to the NEO-Scout to desaturate the reaction wheels in transit as well as to maneuver around the asteroid as previously discussed in Section IV.C. Figure 6 shows the placement of each thruster. Each thruster has a role in translation and rotation. Due to the orientation of the solar panels and engine the placement for thrusters 1 through 8 are at the 80 degree angle. This makes is so the thrust for each of those thrusters had to be split into its components to calculate the translation and rotation in each axis.

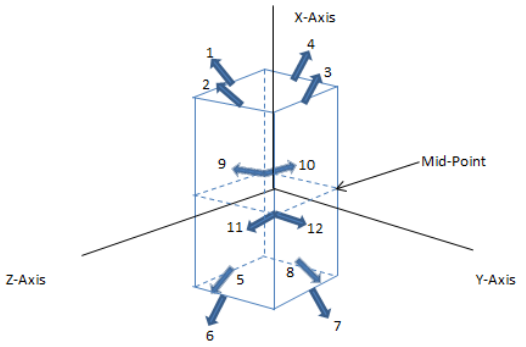

Figure 6. Orientation of cold gas thrusters.

The Marotta Cold Gas Microthruster were chosen as the cold gas thruster for this CubeSat design.[36] Each thruster has a thrust of 0.05 N, an I_{sp} of 65 s, a mass of less than 60 g, and uses N_2 as a propellant. These thruster have an open response time of 5 ms, a close response time of 5 ms, and an ideal operating pressure at 100 psia. The Marotta thruster is flight qualified and was developed for the GSFC Nanosats and the ST-5.[37]

VII. Power Generation and Storage

The onboard subsystems dictate the required power. It was determined the engine needed 600 W for nominal use. In addition, another 50 W needed for the balance of spacecraft operations, control functions, and communications. A PV array of 650 W was chosen to account for a possible degradation of 5% for which the engine would still be able to run nominally with all required in-transit subsystems. The schematic for the Power Control System is shown in Figure 7.[38] The angle between the PV array normal and the Sun vector is calculated during the Hall engine thrusting cycles. The solar arrays are constrained to this vector throughout the burns to maximize power generation. This constraint dictated the rotational degrees of freedom of the solar array to maintain optimal power generation.

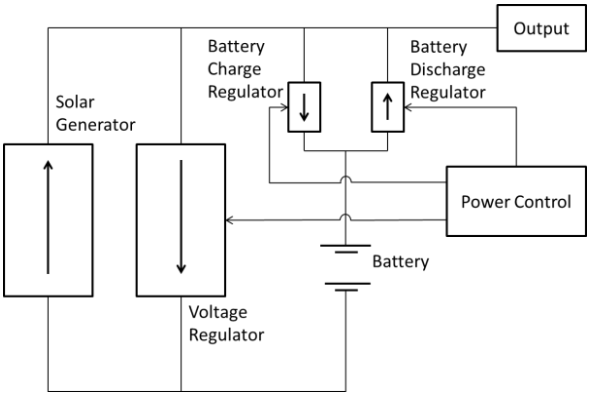

Figure 7. Simple Schematic of Power Generation, Storage, and Distribution System

A. Solar Panels

The Ultra Triple Junction (UTJ) Solar panels with a 6 mil Ceria Doped Coverslide produced by Spectrolab were selected because of a high power per unit mass; 160.2 W/kg.[39] UTJ panels are also currently being mass produced which increases availability of these cells. These panels performs at 27.7% efficiency average at max power and 28℃. This means 4.05 kg of panel area (0.3 m x 7.67m) is required to produce 650 W, providing power for both the Hall Effect engine and the spacecraft subsystems.

B. Battery Power Storage

The battery provides power to the satellite's various internal systems such as payload, attitude, and computing. The design process for the battery was limited by mass and power constraints. Since the solar panels were designed to provide the required output needed for spacecraft operations, the battery provides redundancy in case of eclipse or emergency attitude corrections. Because the satellite is launched from GEO or beyond, the only eclipse possible will occur during asteroid proximity maneuvers. It was determined that the chosen battery would need to supply enough power during minor eclipses to power the cold gas thrusters and payload. The battery selected was GOMSpace NanoPower Flexible Battery Pack BPx series.[40] It is a lithium-ion battery which provides high energy density and little degradation of capacity during repeated charging/discharging cycles.

C. Power Processing Unit

A low mass, high power Hall Thruster system can provide problems for most commercially available solutions. Busek presents a PPU solution under SBIR for their BHT-600 thruster that has a design goal of 2 kg.[25] Becasue the specifications of this PPU are largely unknown, a supplemental, off the shelf CubeSat Power Distribution Module (PDM) available from ClydeSpace was selected to handle the NEO-Scout's lower voltage avionics.[41]

VIII. Thermal Management and Control

The thermal system was designed to be predominantly passive to allows for self-regulation. However, due to the desired range of operation that is required (0.7 AU to 1.3 AU) and the thermal constraints of the Propellant Management System, a completely passive system is difficult to achieve. Hence, a passive system suitable for most conditions was selected with a supplementary active system used for the PMS.

A. Passive System

The temperature requirement for all the instruments was tabulated. From the table generated, it was noted that 0℃ to 60℃ was the desired temperature range for the spacecraft. From here, an energy balance was performed for an open system.[42] The assumption for these calculations was that the spacecraft was a flat plate with a uniform exterior. The design factor solved for was the absorptivity divided by the emissivity. Calculations were performed for several different environments in order to check the extreme temperatures the satellite may encounter. The environments considered were in GEO as well as 0.7 AU, 1 AU, and 1.3 AU away from the Sun. GEO was selected because the Earth emits radiation and reflects the Sun's. 0.7 AU is the closest environment to the Sun that the satellite experiences while 1.3 AU is the farthest. 1 AU provided an average trajectory environment and a reasonable benchmark; however, the satellite must be able to operate at the hot and cold extremes of 0.7 and 1.3 AU, respectively, as dictated by the initial requirements. The final environment considered was around the NEO, however, NEO albedo contribution to the thermal environment were shown to be negligible.

From the data shown in Table 7, the material selected for the external paneling was Aluminized Teflon. This material had an absorbance of 0.2 and an emissivity of 0.8. This allows for the spacecraft to not require an active temperature control system while in GEO or at the hot extreme (at 0.7 AU). From here, the energy equation was then reevaluated and solved for the required watts needed to heat the spacecraft's temperature sensitive components at the cold extremity (1.3 AU). This was calculated to be just over 10 W. This served as one of the requirements for the active system that needed to heat the satellite for any potential trajectories.

A heat sink is included to dissipate energy generated by the electronic subsystems during operation. To prevent mechanical components, a bimetallic spring utilizing metals with high coefficients of thermal expansion will be used to expose the heat sink to the external environment as needed. The heat sink parameters are dictated by the efficiency of the higher power electronic components, especially the Hall effect engine system, and heat flux due to them.

Table 7. Design parameter α/ϵ for each proposed environment.

Location	T, K	$q''_{Sun}, \frac{W}{m^2K^4}$	$q''_{Earth}, \frac{W}{m^2K^4}$	$q''_{Albedo}, \frac{W}{m^2K^4}$	$\sigma, \frac{W}{m^2K^4}$	α/ϵ
GEO	273 - 333	1376.5	230	408	5.67E-8	0.156-0.346
0.7 AU	273 - 333	2809.2	0	0	5.67E-8	0.112 - 0.246
1 AU	273 - 333	1376.5	0	0	5.67E-8	0.229 - 0.507
1.3 AU	273 - 333	814.5	0	0	5.67E-8	0.387 - 0.856

B. Active Heating System

With the implementation of a PMS for iodine, an active heating system is required in order to heat the solid iodine to a usable vapor pressure for the Hall Effect thruster. A conservative estimate of the heated area for the piping and tank was determined to be 1900 cm^2. A power requirement of 65 watts to heat from ambient to operational temperature was established, based on manufacturer sizing estimates.[34] It is estimated that at nominal operating conditions 99% of the subsystems power goes to the thruster and only 1% is used by the heaters.[32] Because the operational temperature of the PMS exceeds the survival range of various electrical components, the PMS must be thermally isolated from the rest of the NEO-Scout with the ability for excess heat to be diverted to the more

temperature sensitive components via conduction and radiation to the avionics based on need.

IX. Communication

Transmitting quality data and images from small spacecraft over interplanetary distances has always been one of the more important challenges facing the spacecraft designer. NEO-Scout will utilize the same telecommunications strategy pioneered by the Deep Space 1 spacecraft which combined limited high-gain, high-rate data telemetry with a low gain, low-rate beacon monitor.[43] The low-gain, low-power beacon monitor transmits one of several tones indicative of overall spacecraft health and the possible need for intervention by operators on the ground. Beacon Monitor technology is aimed at decreasing the total volume of downlinked engineering telemetry by reducing the both the frequency of downlink and the volume of data received per pass. Because the Beacon monitor transmits only one of several carrier sub-frequencies, and not digital data, the signal is relatively easy to recover with modest receiving equipment that employ signal averaging and Fourier Transform techniques.[44] On NEO-Scout, the beacon monitor can be implemented with using one of several commercially available 1 to 2 W CubeSat S-Band transmitters with matching wide beam antennas[45] and on-board Beacon Monitor support software. A complimentary S-Band receiver will also be required to receive low rate telemetry from the ground during contingencies.[46]

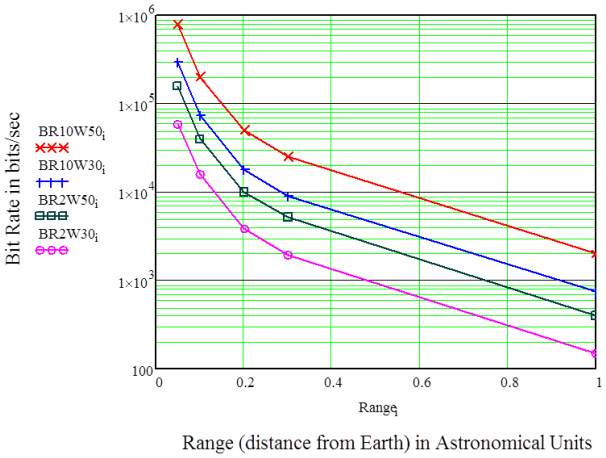

Figure 8. Expected NEO-Scout down link bit rates as a function of distance from Earth in AU for 4 different combination of satellite high gain antenna diameter and satellite X-band transmitter output power; e.g. BR10W50 = 10 W transmitter and 50 cm dish. Use of the 34 meter diameter DSN ground stations is assumed and the link margin is greater than 1 dB is all cases.

The design of the high rate telemetry system for NEO-Scout depends on: 1) the characteristics of the ground stations receiving the data, 2) the characteristics of the high rate data transmitter on the satellite and, 3) the range of acceptable bit rates and corresponding system noise margins.[47] The nominal ground stations selected for this design study are the 34 meter (high gain receiver dish diameter) Deep Space Network receivers.[48] The higher gain (hence higher data rate) 70 M diameter DSN receivers are fewer in number and not as readily available, though much higher data rates are possible if they are.

The core of the NEO-Scout high rate telemetry system is one of the several commercially available 2 Watt CubeSat X-Band transmitters.[49] If needed, transmitter output can be boosted to 10 Watts using commercially available, compact, integrated circuit X-Band linear amplifiers.[50] A complimentary X band receiver will be needed to receive high rate communications from the ground especially during proximity operations around the target NEO.[51]

The results of the link budget[52] analysis for the NEO-Scout downlink is shown as a function of range (i.e. distance from Earth in AU) in Figure 6. Assuming a link margin of 1 dB and a bit error rate of 10^{-6}, the resulting bit rate is calculated for two different NEO-Scout transmitter output powers (2 watts and 10 watts) and two different satellite high gain dish diameters (30 cm and 50 cm). As expected, larger diameter high gain antennas and higher transmitter output power always result in higher bit rates. However, even the 2 watt transmitter/30 cm antenna combination leads to bit rates above 1000 bits/s at ranges less than 0.5 AU. At 0.2 AU the lowest bit rate combination provides 3800 BPS so that a 1 megabit image can be downlinked in about 8 minutes. As can be seen in Figure 6, bit rates increase rapidly between 0.2 AU and 0.05 AU so that the time needed to downlink a 1 megabit image is reduced to 32 seconds for the lowest bit rate combination and 2.4 seconds for the highest bit rate combination both at 0.05 AU.

X. Computing

The Intrepid System Board is an on-board Linux computer designed for CubeSats by Tyvak.[53] It is used for attitude control, data handling, telemetry, and general engine control, all of which are critical systems that require processes handled by a separate chip. The Intrepid is microSD compatible, allowing for data storage from the payload systems and enabling the data to be processed for transfer back to Earth at a later time. This processor also

contains software for the control of reaction wheels based on positioning output from the star tracker discussed previously in the Attitude section. This enables day-to-day autonomy of the NEO-Scout, lowering the power requirement for the transmitter. The Intrepid is equipped to handle the dangers of space, as it has latch-up protection which enables it to detect errors caused by stray particle radiation. It can also accommodate two daughter boards to provide string redundancy for basic avionics.

XI. Guidance, Navigation, and Control

Issues arise regarding the navigation of the NEO-Scout towards its target. Specifically, knowledge of the positions and velocities of the spacecraft, Earth, Sun, and asteroid are crucial throughout the mission. The data is needed for both orbit determination and flight path control. For a given trajectory, communication with Earth, solar panel angle, engine burn timing, and payload orientation are all functions of the craft's position relative to the Earth, Sun, the fixed stars and the target asteroid.

Spacecraft position and velocity are determined against the background of fixed stars by the star tracker discussed previously in Section VI. The inputs from the star tracker are used to locate the position of the NEO-Scout relative to the Sun and Earth for solar power generation and telemetry respectively. During the transfer orbit from the Earth to the target asteroid, the orientation of the spacecraft is driven by the desired thrust vector and the position of the spacecraft relative to the Sun. The desired orientation is to have the X_{body} vector in line with the thrust and to have the Y_{body} vector perpendicular to the position vector relative to the Sun. This greatly limits the availability of high-gain telemetry during this phase of the mission profile. The low-gain omnidirectional beacon monitor antenna offers one solution to the pointing conflict by allowing for low bit rate telemetry regardless of the orientation of the craft relative to the Earth reference vector. The high gain X-Band telemetry system can be used by interrupting Hall thruster operations and pointing the high gain antenna at Earth to acquire range-rate data and then reorienting the spacecraft to resume thruster operations. The telemetry system in combination with the star tracker are the primary guidance navigation and control instruments for the transit phase of the mission, employing a combination of well-known optical and radio frequency methods with data downlink via the DSN 34 meter diameter dish receivers.[54]

The exact timing, magnitude, duration, and direction for the transfer orbit are functions of the trajectory plan, which varies along with the desired mission. Ion engines are typically operated with long burns due to the complexity associated with initiating thrust and propellant flow. The exact thrusts and flow rates desired can forseeably be changed throughout the mission; however, the thrust is constrained by the electric power available. The timing and direction of the burn of the main engine depends on the type of orbit change desired at the time (e.g., inclination change, apse line rotation) as well as the magnitude of the change. For the transfer orbit detailed in Table 3, the main propulsion engine operates for three separate burns at a nominal thrust of 39 mN.

For proximity operations within a few hundred meters of the asteroids surface, the payload instruments require pointing information and the spacecraft operators need information on the character of the primary orbit around the asteroid and how that orbit is changing with time. The asteroid's position and apparent movement with respect to the spacecraft is determined using the radar altimeter or laser range finder included in the payload in combination with the primary camera. This information is used to determine the asteroid's relative position, shape and apparent rate of movement relative to the spacecraft. The computing power of the NEO-Scout is limited; therefore, high rate telemetry is required for ground stations to determine the spacecraft orbit around the target asteroid and the rate of change of that orbit with time. This requires the NEO-Scout to point the dish (Z_{body} axis) along the position vector relative to Earth. Once the spacecraft distance and primary orbital characteristics have been determined, proximity operations can commence. The spacecraft position sensor points at the asteroid along the X_{body} vector and provides feedback to the controller in the CPU. This interfaces with the cold gas thrusters in order to lower the orbit or attempt to guide the spacecraft to a controlled impact with the asteroid using the boom-extended accelerometer with the surface of the asteroid in such a way as to not damage the NEO-Scout. Soon after the impact, the NEO-Scout thrusts away from the asteroid and maneuvers again for telemetry.

Station keeping maneuvers are operated in a similar manner to the main transfer orbit. That is, the maneuvers are dependent upon the trajectory and the spacecraft's orientation. Minor station keeping maneuvers may be accomplished through the use of the craft's reaction wheels; cold gas thrust system, and main engine gimballing. Larger station keeping maneuvers may be accomplished through spacecraft orientation changes and longer duration main engine burns.

XII. Payload

Instrument selection is driven primarily by the payload mass budget, as well as launch and environmental survivability requirements. A payload mass budget of 2.2 kg is anticipated, but uncertain, as payload mass is dependent and must accommodate changes in the mass requirements of other modules. As such, instruments that

make effective use of mass towards measurement objectives are proposed in Table 9. Limited data rates will further restrict payload selection, favoring instruments with fewer data bits per sample, and instruments which require fewer samples to meet measurement objectives.

Table 9. Proposed Instruments

Name	Measurements	Mass (kg)
FLIR MLR-2k[55]	Distance to Object	0.115
NanoCam C1U[56]	Visible Imaging: Size, Appearance, Albedo	0.166
FLIR Tau SWIR[57]	Near IR Imaging: Size, Appearance, Albedo	0.131
FLIR Quark 640 + 35mm[58]	Thermal IR Imaging: Surface Temperature Distribution	0.028
Surface Penetrator (TBD)[59]	Mechanical Impact Properties	0.5
Miniature Radar Altimeter T2[60]	Surface Profile	0.375
Argus 1000 IR Spectrometer[61]	Composition: Si, C, Other Simple-Element Bonds	0.23
Compact Neutron Albedo Instrument[62]	Water, Hydrogen, Trapped Volatiles	0.5
Alpha Proton Spec. (TBD)[63]	Composition: Light elements, Na, Al, Mg, Si, S	0.5

With a payload mass budget of 2.2 kg, the first eight instruments are proposed, making ~10% of total payload mass available for conduits and mounting. As the exclusive instrument used to measure mechanical properties, and only non-optical instrument, the Surface Penetrator is unique. The penetrator would feature an ejection system, a compound accelerometer to record impact behavior, and a detachable tether to relay data to the NEO-Scout. Without the tether, a transmitter-receiver pair is required, increasing mass and risk. Alternately, NEO-Scout can be equipped with a deployable contact boom and use internal accelerometers to determine NEO surface resistance when the probe contacts the surface during a slow spacecraft approach.

Imaging devices will record the NEO size, albedo, appearance, and surface temperature distribution. Spectrometers will record NEO material composition. To minimize volume and maximize utility, integrated optics systems similar to Deep Space 1's MICAS[64] are being considered to replace multiple imaging and spectrometry devices. Should the payload mass budget support more comprehensive measurement of surface composition, Laser Induced Breakdown Spectroscopy provides unique advantages which may be better suited for this application. This technology has been demonstrated in space missions, and is being redesigned to minimize mass for military field use. Military field units may be adaptable, as they are slightly over 2 kg and designed to be durable through shock and vibration, but may need further modification for space flight thermal and radiation environments.

Some of the instruments in the above table have flight heritage in LEO and present lower risk in the interplanetary flight environment. Others are COTS items manufactured for civilian or military use in earth surface environments and must be viewed as functional prototypes of units suitable for space flight. The corresponding space flight units will need to be developed using the COTS functional prototypes as a starting point. The spaceflight thermal and ionizing radiation environments present the most important risk items with respect to the COTS instruments listed.

Instruments will require additional testing and modification to survive these conditions. Further, some instruments have not been demonstrated to survive launch loads. To anticipate these costs a factor of roughly 10x is applied to instrument vendor prices of COTS payload instruments with and without LEO flight heritage.

XIII. Final NEO-Scout Design Summary

Table 10. Spacecraft mass power telemetry and other characteristics here with comparison to design objectives in Table 1.

	Design Criteria	Achieved Metrics
Dry Mass range	< 20 kg	15 kg
Wet Mass range	< 35 kg	24.5 kg
Delta V range	< 10 km/s	7.68 km/s
Maximum Mission Duration	100 to 400 days	345 days
Maximum Distance to Earth at Rendezvous	0.3 AU	0.18 AU
Maximum Telemetry Range	0.3 AU	0.3 AU
Minimum Telemetry Data Rate	2000 to 10000 Bps	2000 Bps
Spacecraft Cost	$15M	$15-25M

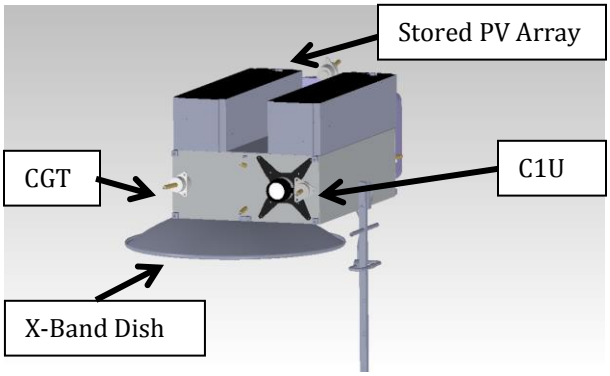

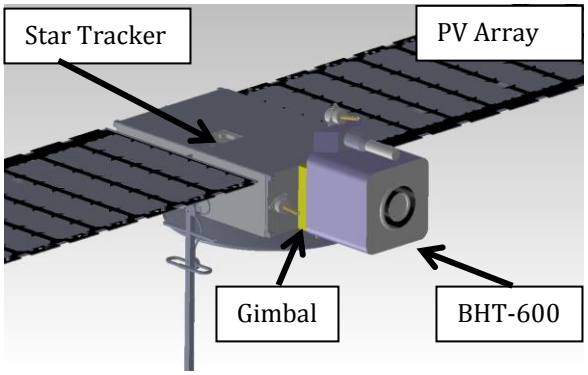

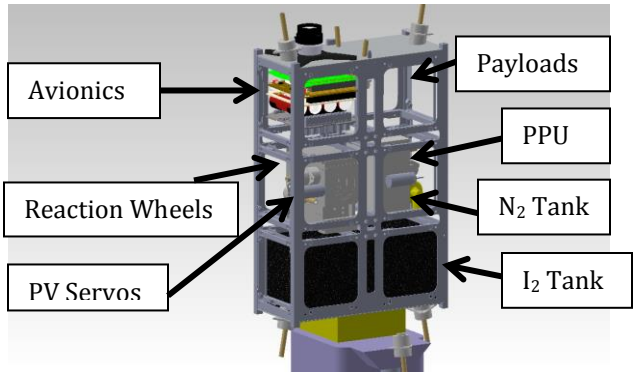

Figure 9a (upper left). Shows the undeployed NEO-Scout.
Figure 9b (above). Shows the deployed external view of the NEO-Scout.
Figure 9c (left). Shows the internal placement of various components.

Table 11 (below). Final spacecraft mass and peak power consumption by subsystem. Note that the total peak power consumption exheeds the designed power generation; however, not all systems are required to operate concurrently. The estimated peak power consumption for the NEO-Scout is less than 650 W.

Subsystem	Mass, kg	Peak Power Consumption, W
Attitude	1.714	3
Propulsion	1.246	600
Power Management	6.35	15
Structural	1.977	0
Communication	1	18
Computing	0.055	.25
Fuel	9.5	20
Payload	2.2	77.2
Total	24.5	733.45

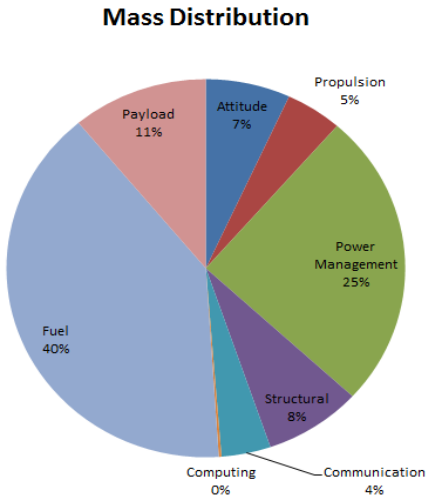

Figure 10. Shows the mass distribution of each subsystem as a percentage.

XIV. NEO-Scout Cost Model

Existing "small" space project cost models, like the Aerospace Corporation Small Satellite Cost Model (SSCM)[65] are based on historical cost data from satellite projects substantially larger than contemporary CubeSat projects including the one proposed here, however the model has been used successfully for NEO-Scout sized spacecraft projects.[66] Spacecraft buss dry mass and the spacecraft complexity indies are the most important SSCM input parameters so that with a NEO-Scout launch mass of less than 40 kg and a complexity index estimated at 0.4, total spacecraft cost, including development, is conservatively estimated at between $15M and $25M for the first flight demonstration unit.

Recent CubeSat based micro/nano satellite programs have reported cost figures in the same range or even lower.

For example, the Boeing Phantom Phoenix Nano, a 3U CubeSat LEO bus with two string redundant avionics system and a 1.83 kg payload capacity, is commercially available for about $2M to $3M. NASA Ames Research Center has successfully flown a number of 1 U to 3 U LEO flight programs at total program costs on the order $10M and development times on the order of 12 months. Several commercial suppliers offer 3U cube sat systems with single string avionics systems for total purchase prices less than $1M.

Many of the commercial CubeSat components and payload instruments described above have considerable flight heritage in LEO, however, some do not. Even those with extensive flight heritage in LEO have not been demonstrated beyond LEO. Exposure to galactic cosmic rays and solar particle events is increased beyond LEO. CubeSat hardware and payload instruments will require additional testing and likely modification to assure reliable operation in the interplanetary flight environment. As a result, the basic NEO scout hardware cost is multiplied by a factor of 10 to account for expected hardware testing and modification costs as well as assembled spacecraft qualification and acceptance testing.

XV. Risk Management

In-flight failure of avionics components, especially integrated circuits, has been an important concern for spacecraft designers since the beginning of the space age.[67] A key feature of the CubeSat technology is the extensive use of commercial electronic parts (COTS) that exhibit high performance and relatively low procurement cost but introduce mission success risks that result from possible increased failure rates in the space flight environment.[68] Successful flight in LEO demonstrated reduced risk but some residual risk remains for interplanetary flight because the ionizing radiation environment is somewhat more severe. COTS avionics mission success risks are managed for the NEO-Scout vehicle by using several risk mitigation methods.

A. Space Radiation risks to avionics and payload instruments.

First, not all COTS components are created equal. Selection of components manufactured to higher reliability standards with some radiation resistance based on device architecture and materials will reduce the mission success risk. Second, testing early and testing often will weed out high risk components and further reduce mission success risk. Thermal vacuum testing and ionizing radiation effects screening tests are most important here. Ionizing radiation testing should focus both on total ionizing dose and single event phenomena. Finally, International Space Station facilities can be exploited to perform long term (1 year or more) supplementary qualification testing of NEO-Scout sub-assemblies. While the LEO ionizing radiation environment at ISS is less severe than the interplanetary environment, the differences are quantitative not qualitative so that scaling single event rates from LEO to the interplanetary environment offers useful risk assessment and mission success probability estimates. The nominal single event environment has been well characterized in both environments and in-flight single event rates predicted with accuracy sufficient for spacecraft verification work in both environments .[69] It should be remembered that there is no simple hardware acceptance test for ionizing radiation. All such testing is essentially destructive to the qualification test article. For that reason, electronic parts procurement and inventory control is a vitally important aspect of overall risk reduction because qualification testing is valid if and only if it can be shown that the flight articles are sufficiently similar to the qualification test article.

The interplanetary solar particle event environments are not directly available for testing hardware on ISS as a result of geomagnetic shielding, though some indication of resistance to solar particle event effects are provided by passage through the South Atlantic Anomaly, a low altitude extension of Earth's inner proton belt.

B. Solar Particle Event Shielding

Solar particle events exhibit a wide range of intensity and duration and have been the subject of studies focused on total ionizing dose reduction by shielding mass and in-flight single event effect rate increases in interplanetary spacecraft avionics.[70] Fortunately, the kinetic energy spectrum of solar particle event protons is much softer than galactic cosmic rays so that significant mitigation of both total ionizing dose and single event effects is achievable with reasonable amounts of shielding mass.[71]

It is important to ensure that the electronics and circuitry of the spacecraft possesses proper shielding for at least one solar particle event (SPEs). According to Jackman,[72] Geostationary Operational Environmental Satellites have measured SPE protons with energies greater than 100 MeV, although 85% of the protons in space have energies of 1-10 MeV.[73] Nevertheless, 100 MeV was chosen as the worst-case scenario for analysis.

A commonly-used parameter to measure the decelerating force of subatomic particles traveling through a certain material is the stopping power of the material. For the purposes of this analysis, it is measured in MeV per cm of the material. The Bethe stopping formula[74] expresses this value according to the energy of the penetrating proton:

$$S = \frac{4\pi {e_1}^2 e^2}{mv^2} {Z_2}^2 \ln\left(\frac{2mv^2}{I}\right) \quad (1)$$

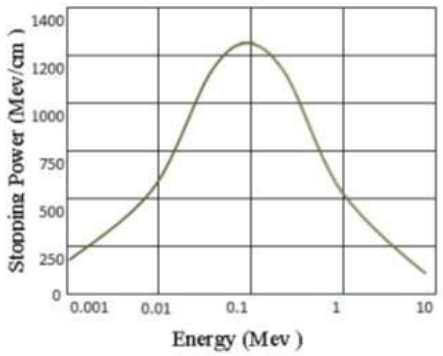

Figure 11. Stopping Power of Aluminum over a range of Single Particle Event intensities.

Aluminum plating was chosen as the shielding material for this proposal due to its high availability and low cost. The results of the Bethe stopping formula for aluminum are shown in Figure 11 for protons in the range of 0.001-10 MeV.[76]

From this data, it can be seen that, at the normal maximum of 10 MeV, aluminum exhibits a stopping power of 100 MeV/cm, so a minimum thickness of 1 mm is required for the aluminum shielding. However, it can be estimated from the above figure that for a worst case of an event of 100 MeV, stopping power could be as small as 50 MeV/cm, requiring shielding of a 2 cm thickness. Due to weight constraints, 1 mm plating will be used. Since the avionics equipment, which is sensitive to particle events, will be located in the top two CubeSat units, the plating will be applied to the 10 outer faces of those units.

XVI. Conclusions

The proposed NEO-Scout successfully meets all mission requirements set forth and demonstrates several proofs of concept important for future designs. The NEO-Scout can intercept NEOs as they pass close to the Earth moon system with mission times in the range of 100 to 400 days.

The NEO-Scout demonstrates the effectiveness of the Hall engine and the usefulness of iodine as a potential fuel source for future CubeSat missions thanks to its high storage density and low storage pressure. It also demonstrates the fuel management system for iodine. This new fuel system allows the Scout to reach asteroids without the additional weight complexity and risk presented by high pressure xenon gas handling systems. The flight time is limited to around a year in order to minimize the risk of long term avionics exposure to the interplanetary flight environment. The Scout is designed to survive 80% solar particle events through aluminum by using supplemental shielding against energetic solar protons and careful selection/up-screening of COTS avionics components.

Once at the asteroid, the Scout can maneuver using cold-jet thrusters to obtain vital data about the dimensions and composition of the asteroid through visible imaging, surface contact to evaluate surface mechanical properties, near and far IR imaging and near infrared spectroscopy. Once the data is collected, the Tyvak flight computer processes this data and either transmits it immediately, or stores it for later transmission.

Effectively communicating with Earth over a long distance is a challenge for a CubeSat based design due to the size and power constraints compared to typical satellite. The Scout deals with these issues by both bolstering the power devoted to communication and by using a 60cm dish to ensure minimal data loss over great distances.

To meet the NEO-Scout's need for power, one externally attached panel was needed. A single panel was used to reduce mechanical components as well as to avoid the deployed communication dish. Additionally, by allowing the panel to rotate axially, solar energy incidence is maximized and the reaction wheel workload is minimized.

In order to counteract the extreme temperature fluctuations in space, Aluminized Teflon was chosen as the NEO-Scout passive thermal control material. This isolates the need for an active temperature control system to the iodine fuel management system alone. Any heat generated by this active system can be directed to other components, if needed.

The NEO-Scout is a low-cost solution to the problem of characterizing a significant number of object in the NEO population at relatively low cost. As opposed to a single Discovery class mission, multiple NEO-Scouts can be sent out to multiple asteroids to collect data vital for selecting targets and planning operations for more ambitious and costly missions. The NEO-Scout also demonstrates the advantages of a working iodine fuel system for Hall Effect thruster that is more efficient and safer than conventional high pressure xenon systems. The NEO-Scout is a possible model of future interplanetary CubeSat spacecraft.

Appendix

Table 12. Potential Target asteroids that met the system requirements outlined in Table 1 and also are compatible with the NEO-Scout configuration outlined in this paper. The analysis done in this paper was for 2007 SQ6 (bold).

Asteroid Name	e	a, AU	i, deg	Minimum distance, AU	Total delta V, km/s	Size, m	Earth Departure	Duration, days
2006 EW52	0.09568	1.24575	8.882	0.14336	5.82	101-226	8/28/2023	304
2012 DT60	0.11256	1.19184	7.48462	0.1126	5.19	101-226	9/15/2024	128
1996 XB27	0.05794	1.18872	2.46456	0.11494	4.88	106-237	9/26/2022	240
2007 SQ6	0.14553	1.04299	9.10124	0.00982	5.35	111-248	9/29/2023	96
2011 UV63	0.13405	1.19303	9.78502	0.03441	5.12	121-272	3/28/2020	288
2006 KL21	0.12754	1.19923	9.35515	0.04767	6.36	176-393	7/24/2022	352
2011 AM24	0.14974	1.17824	9.1351	0.0092	4.67	221-494	7/29/2024	256
1991 JW	0.11866	1.03913	8.70995	0.02068	6.96	335-748	6/9/2023	304
1989 ML	0.13649	1.27211	4.37825	0.08155	5.14	367-820	7/8/2022	320

References

[1]3rd Interplanetary CubeSat Workshop, URL: http://icubesat.org/ [cited 6 April 2014].

[2]AIAA/USU Conference on Small Satellites, URL: http://digitalcommons.usu.edu/smallsat/ [cited 6 April 2014].

[3]Staehle, R. L., et al., "Interplanetary CubeSats: Opening the Solar System to a Broad Band Community at Lower Cost," *Journal of Small Satellites* [online journal], Vol. 2, No. 1, URL: http://www.jossonline.com/Papers.aspx?id=ftu84kjc [cited 6 April 2014].

[4]Conversano, R. W., and Wirz, R. E., "Mission Capability Assessment of CubeSats Using a Miniature Ion Thruster," *Journal of Spacecraft and Rockets*, AIAA Journal, Vol. 50, No. 5, 2013, pp. 1035-1046.

[5]"Target NEO: Open Global Community NEO Workshop Report," *Proceedings of the Open Global Community NEO Workshop*, edited by B. Barbee, George Washington University, Washington D. C., 2011.

[6]McFadden, L. A., Binzel, R. P.; Near Earth Objects, Chapter 14, Encyclopedia of the Solar System, Academic Press, New York, 2007, pp 283-300.

[7]Rivkin, A. S.; "An Introduction to Near-Earth Objects," *Johns Hopkins APL Technical Digest*, 27(2), 2006, pp 111-120.

[8]"Near Earth Object Program," *National Aeronautics and Space Administration* [online database], URL: http://neo.jpl.nasa.gov/ [cited 6 April 2014].

[9]"NEO Earth Close Approaches," *National Aeronautics and Space Administration* [online database], URL: http://neo.jpl.nasa.gov/ca/ [cited 6 April 2014].

[10]"Near-Earth Object Human Space Flight Accessible Targets Study," *National Aeronautics and Space Administration* [online database], URL: http://neo.jpl.nasa.gov/nhats/ [cited 6 April 2014]

[11]Landau, D., Strange, N., "Near Earth Asteroids Accessible to Human Exploration with High Power Electric Propulsion", *Proceedings of the AAS/AIAA Astrodynamics Specialist Conference*, paper AAS 11-146, July 31-August 4, 2011, Girdwood, Alaska.

[12]Lee S., Hutputanasin A., Toorian A., and Wenschel Lan W., "CubeSat Design Specification." California Polytechnic State University, San Luis Obispo, CA

[13]Karmer, H. J., "CubeSat Concept," *eoPortal Directory* [online encyclopedia], URL: https://directory.eoportal.org/web/eoportal/satellite-missions/c-missions/cubesat-concept [cited 8 April 2014].

[14]"Hayabusa," *Encyclopedia Astronautica* [online encyclopedia], URL: http://www.astronautix.com/craft/hayabusa.htm [cited 6 April 2014].

[15]Olds, J. R., Charania, A.C., and Koenig, J., "Foresight: Designing a Radio Transponder Mission to Near Earth Asteroid Apophis," *IAA Planetary Defense Conference*, 28 April 2009, URL: http://www.sei.aero/eng/papers/uploads/archive/IAAPD2009_1544473.pdf [cited 4 April 2014]

[16]Systems Tool Kit. Software Package, Vers. 10.1. Analytical Graphics, Inc., Exton, PA, 2013.

[17]"NEAR Mission Profile," *National Space Science Data Center* [online database], URL: http://nssdc.gsfc.nasa.gov/planetary/mission/near/near_traj.html [cited 6 April 2014].

[18]Kahn, E.G., Barnouin, O.S., et al, "Improved Estimation of the Hayabusa SpaceCraft Trajectory and Lidar Tracks," 2012, 1648-1649, URL: http://www.lpi.usra.edu/meetings/lpsc2012/pdf/1648.pdf [cited 18 March 2014].

[19]Kuninaka, H., Nishiyama, K., et. al., "Hayabusa Asteroid Explorer Powered by Ion Engines on the way to Earth," *Proceedings of the 31st International Electric Propulsion Conference*, Michigan, USA. 2009.

[20]Sutton, G., and Biblarz, O., *Rocket Propulsion Elements*, 8th ed., John Wiley & Sons, Inc., Hoboken, NJ, 2010.

[21]Szabo, J., et al. "Performance Evaluation of an Iodine-Vapor Hall Thruster," *Journal of Propulsion and Power* Vol 28.4, 2012, pp. 848-857.

[22]Kieckhafer, A., and King, L.B., "Energetics of Propellant Options for High-Power Hall Thrusters," *Proceedings of the Space Nuclear Conference*, San Diego, CA, 2005.

[23]"Hall Effect Thrusters," *Busek Space Propulsion and Systems*, [manufacturer website], URL: http://www.busek.com/technologies__hall.htm [cited 8 April 2014].

[24]"Hall Effect Thrusters," *Alta* [manufacturer website], URL: http://www.alta-space.com/index.php?page=electric-propulsion [cited 8 April 2014].
[25]"Low Mass Low Power Hall Thruster System," *Small Business Innovation Research* [online database], URL: https://www.sbir.gov/sbirsearch/detail/369381 [cited 8 April 2014].
[26]Lobbia, R.B., and Gallimore, A.D., "Performance Measurements from a Cluster of Four Hall Thrusters," *Proceedings of the 30th International Electric Propulsion Conference*, Florence, Italy, 2007.
[27]Bui, D.M., "Plume Characterization of Busek 600W Hall Thruster," Thesis, Air Force Institute of Technology, Wright-Patterson Air Force Base, OH, 2012.
[28]Oslyak, S., et al. "Characterization of an Adjustable Magnetic Field, Low-Power Hall Effect Thruster", *Proceedings of the 32nd International Electric Propulsion Conference*, Wiesbaden, Germany, 2011
[29]"COBRA Gimbal," *Tethers Unlimited* [online datasheet], URL: http://www.tethers.com/SpecSheets/Brochure_Gimbal.pdf [cited 8 April 2014].
[30]Dankanich, John W., Hani Kamhawi, James Szabo and Bruce Pote, "Iodine Electric Propulsion for Interplanetary Small Satellite Applications," *2013 Interplanetary Small Satellite Conference* [online database], URL: http://www.intersmallsatconference.org/2013/docs2013/C.2.2_Dankanich_Presentation.pdf [cited April 6 2014].
[31]"Kapton Heaters," *TEMPCO Electric Heater Corporation* [online datasheet], URL: http://www.tempco.com/Catalog/Section%209-pdf/Foil%20Heaters.pdfEMPCO Flexible Heaters [cited 8 April 2014].
[32]Hillier, A. C., "Revolutionizing Space Propulsion through the Characterization of Iodine as fuel for Hall Effect Thrusters," Thesis, Air Force Institute of Technology, Wright-Patterson Air Force Base, OH, 2011.
[33]Szabo, J., Mike R., Surjeet P., Bruce P., Vlad H., Chas F.. "Iodine Propellant Space Propulsion," *Proceedings of International Electric Propulsion Conference*, Washington D.C., October 2013.
[34]Nakles, M. R., Brieda L., Hargus Jr., W. A., Spicer R. L., "Experimental and Numerical Examination of the BHT-200 Hall Thruster Plume," *43rd AIAA/ASME/SAE/ Joint Propulsion Conference & Exhibit* [online database], URL: http://arc.aiaa.org/doi/abs/10.2514/6.2007-5305 [cited April 6 2014].
[35]"BCT XACT," *Blue Canyon Technologies* [online datasheet], URL: http://bluecanyontech.com/wp-content/uploads/2012/07/BCT-XACT-datasheet-1.5.pdf [cited April 6 2014].
[36]"Cold Gas Microthruster," *Marotta* [manufacturer website], URL: http://www.marotta.com/fluid-control-building-blocks/cold-gas-microthruster.html [cited 8 April 2014].
[37]Mueller, J., Hofer, R., and Ziemer, J., "Survey of Propulsion Technologies Applicable to Cubesats," *NASA JPL* [online database], URL: http://trs-new.jpl.nasa.gov/dspace/bitstream/2014/41627/1/10-1646.pdf [cited 9 April 2014].
[38]Maini, Anil Kumar., and Varsha Agrawal. *Satellite Technology: Principles and Applications*. Chichester: John Wiley, 2007. Print.
[39]"Space Solar Panels," Spectrolab [online datasheet], URL: http://www.spectrolab.com/DataSheets/Panel/panels.pdf [cited 8 April 2014].
[40]"Nano Power BP4 Series," *GomSpace* [online datasheet], URL: http://gomspace.com/documents/GS-DS-BP4-series-1.6.pdf [cited April 6 2006].
[41]"CubeSat Power Distribution Module," *Clyde Space* [online datasheet], URL: http://www.clyde-space.com/cubesat_shop/power_distribution_and_protection/95_cubesat-power-distribution-module
[42]Kaminski, D. and Jensen M. K., *Introduction to Thermal and Fluids Engineering*. Hoboken, NJ: Wiley, 2005. Print.
[43]Taylor, J., Fernandez, M. M., Alamanac, A., B., Cheung, K., M.,; "Deep Space 1 Telecommunications," NASA, JPL, California Institute of Technology, Pasadena, California, 2001
[44]DeCoste, D., Finley, S. G., Hotz, H. B., Lanyi, G. E., Schlutsmeyer, A. P., Sherwood, R. L., Sue, M. K., Szijjarto, J., Wyatt, E. J.; "Beacon Monitor Operations Experiment DS-1 Technology Validation Report," Jet Propulsino Laboratory, California Institute of Technology, Pasadena California, 91109,
[45]"ISIS TXS S-Band Transmitter," *CubeSatShop* [online datasheet], URL: http://www.cubesatshop.com/index.php?page=shop.product_details&flypage=flypage.tpl&product_id=9&category_id=5&option=com_virtuemart&Itemid=67
[46]"Satellite Products," *Innovative Solutions In* Space [online supplier], URL: http://www.isispace.nl/cms/index.php/products-and-services/products [cited April 19, 2014]
[47]Doody, D.; Deep Space Craft Chapter 1, Telepresence, Springer, Berlin, Heidelberg, New York, 2009, ISBN 978-3-540-89509-1
[48]"Deep Space Network," NASA JPL [online database], URL: http://deepspace.jpl.nasa.gov/ [cited April 19, 2014]
[49]"EXC 27 HDR X Band Transmitter," Syrlinks [online datasheet], URL: http://www.syrlinks.com/en/products/cubesats/hdr-x-band-transmitter.html [cited April 19, 2014]
[50] "X Band 10W High Power Amplifier GaAs MMIC," *RFMD* [online datasheet], URL: http://www.rfmd.com/CS/Documents/RFHA5966ADS.pdf [cited April 19, 2014]
[51]No COTS CubeSat X-Band receivers have been identified to date – this will be a custom build or commands will be uplinked via the S band beacon system.
[52]"Basics of Space Flight," *NASA JPL* [online resource], Section II, Chapter 10: Telecommunications, URL: http://www2.jpl.nasa.gov/basics/bsf10-1.php [cited April 19, 2014]
[53]"Intrepid Pico-Class CubeSat System Board," *Tyvak* [online datasheet], URL: http://tyvak.com/intrepidsystemboard/ [cited April 6 2014].
[54]"Basics of Space Flight," *NASA JPL* [online resource], Section II, Chapter 13: Spacecraft Navigation, URL: http://www2.jpl.nasa.gov/basics/bsf13-1.php [cited April 19, 2014]

[55]"MLR-2K Laser Rangefinder," FLIR Electro-Optical Components, [online datasheet], 2013, Issue 1, Rev. 1, URL: http://www.flir.com/uploadedFiles/CVS_Americas/Cores_and_Components_NEW/Products/Components/Laser_Products/FLIR-MLR2K-Datasheet.pdf [cited 9 April 2014].
[56]"NanoCam C1U Datasheet," GomSpace, [online datasheet], 2011, Issue 6, Rev. 1, URL: http://gomspace.com/documents/GS-DS-NANOCAM-6.1.pdfs. [cited 9 April 2014].
[57]"Tau SWIR 25 Miniature High-Performance Shortwave Infrared Camera," FLIR Electro-Optical Components, [online datasheet], 2013, URL: http://cvs.flir.com/tau-swir-25-datasheet. [cited 9 April 2014].
[58]"Longwave Infrared Thermal Core Camera," FLIR Electro-Optical Components, [online datasheet], 2013, URL: http://cvs.flir.com/quark-brochure [cited 9 April 2014]
[59]Galeev, A. A., and Zakharov, A. V., "Mars 96 Penetrator," *NASA-NSSDC* [online database], URL: http://nssdc.gsfc.nasa.gov/nmc/spacecraftDisplay.do?id=MARS96E [cited 8 April 2014].
[60]Webb, P., "Miniature Radar Altimeter," Roke Manor Research Limited, Hampshire, UK, [online datasheet], 2013, URL: http://www.roke.co.uk/resources/datasheets/mra-type-2.pdf [cited 9 April 2014].
[61]"Argus 1000 Infrared Spectrometer," *CubeSatShop.com* [distributor website], URL: http://www.cubesatshop.com/index.php?page=shop.product_details&flypage=flypage.tpl&product_id=91&category_id=16&option=com_virtuemart&Itemid=80 [cited 8 April 2014].
[62]Mitrofanov, I., "Dynamic Albedo of Neutrons (DAN)," *NASA-JPL MSL Science Corner* [online database], URL: http://msl-scicorner.jpl.nasa.gov/Instruments/DAN/ [cited 8 April 2014].
[63]"Mars Pathfinder Science Results," *NASA-JPL Mineralogy and Geochemistry* [online database], URL: http://mars.jpl.nasa.gov/MPF/science/mineralogy.html [cited 8 April 2014].
[64]Soderblom, L., et al., "Miniature Integrated Camera Spectrometer (MICAS)," *Technology Validation Symposium*, Pasadena, CA, February 2000.
[65]"Small Satellite Cost Model," *The Aerospace Corporation [online technical model]*, URL: https://www.aerospace.org/expertise/technical-resources/small-satellite-cost-model/ [cited April 19, 2014].
[66]Bearden, D. A., "Small-Satellite Costs," Crosslink, pp 33-44, Winter 200/2001, Aerospace Corporation, El Segundo California.
[67]Tafazoli, M.; "A study of on-orbit spacecraft failures," Acta Astronautica, 64, (2009) 195-205
[68]Maurer, R. H., Fraeman, M. E., Martin, M. N., Roth, D. R.; "Harsh Environments: Space Radiation Environments, Effects, and Mitigation," *Johns Hopkins, APL Technical Digest*, Vol. 28, No. 1, 2008.
[70]Koontz, S. L., Reddell, B., Boeder, P.; "Calculating Spacecraft Single Event Environments with FLUKA," *Proceedings of the 2011 IEEE Radiation Effects Data Workshop*, Las Vegas, Nevada, July 25-29, 2011, pp 188-195.
[71]Koontz, S., Atwell, W., Reddell, B., Rojdev, K.; "Spacecraft Solar Particle Event shielding," NASA/TP-2010-216-33, Sept, 2010.
[72]Jackman, Charles. "The Influence of Large Solar Proton Events on the Atmosphere," 2012 SORCE Science Meeting [online database], URL: http://lasp.colorado.edu/sorce/news/2012ScienceMeeting/docs/presentations/S2-04_Jackman_SORCE_SPEs_shown_NEW.pdf [cited on 6 April 2014].
[73]Masti, D., Gandomkar, S., and Zeynali O., "Shielding protection of electronic circuits against radiation effects of space high energy particles," *Advances in Applied Science Research*, Vol. 3 ,Issue 1, 2012, p446.
[74]Sigmund, P., *Particle Penetration and Radiation Effects.* Berlin: Springer, 2006.